

Electron-electron interactions in a one-dimensional quantum-wire spin filter

P. Devillard,¹ A. Crépieux,² K. I. Imura,³ and T. Martin²

¹*Centre de Physique Théorique, Université de Provence, Case 907, 13331 Marseille Cedex 03, France*

²*Centre de Physique Théorique, Université de la Méditerranée, Case 907, 13288 Marseille Cedex 9, France*

³*Condensed Matter Theory Laboratory, RIKEN, 2-1 Hirosawa, Wako, Saitama 351-0198, Japan*

(Received 7 January 2005; revised manuscript received 1 April 2005; published 25 July 2005)

The combined presence of a Rashba and a Zeeman effect in a ballistic one-dimensional conductor generates a spin pseudogap and the possibility to propagate a beam with well-defined spin orientation. Without interactions, transmission through a barrier gives a relatively well-polarized beam. Using renormalization group arguments, we examine how electron-electron interactions may affect the transmission coefficient and the polarization of the outgoing beam.

DOI: [10.1103/PhysRevB.72.041309](https://doi.org/10.1103/PhysRevB.72.041309)

PACS number(s): 73.23.-b, 72.25.Dc, 72.25.Mk, 71.70.Ej

Over the last decade, spintronics¹ has emerged from mesoscopic physics and nanoelectronics as a field with implications in both quantum information theory² and for the storage of information. While the charge is routinely manipulated in nanoelectronics, the issue here is to exploit the spin degree of freedom of electrons. In particular, spin filters are needed to control the input and the output of spintronic devices. A recent proposal³ explained the operation of a spin filter for a one-dimensional (1D) wire under the combined operation of Rashba spin orbit coupling and Zeeman splitting. Yet, electronic interactions in one-dimensional wires are known to lead to Luttinger liquid behavior and to the renormalization of scattering coefficients. It is, therefore, important to inquire about the role of electronic interactions in the above-mentioned spin filter. This is aim of the present paper.

A decade ago, a transistor based on the controlled precession of the electron spin due to spin-orbit coupling was proposed.⁴ Indeed, the Rashba effect⁵ in a semiconductor can be modulated by a gate voltage, which controls the asymmetry of the potential well that confines the electrons. Since this proposal, many spintronic devices based on the Rashba effect have been proposed, based on a single electron picture.⁶⁻⁹ At the same time, one-dimensional wires are now available experimentally. This has motivated several efforts¹⁰ to study the interplay between the Rashba effect and electron interactions in infinite one-dimensional wires. However, little has been said about Coulomb interactions in spintronic devices. Our starting point stems from the fact that Rashba devices are gated devices, in which the interaction are assumed to be screened and weak. We will, therefore, use a perturbative renormalization group treatment of the Coulomb interaction in order to address its consequence on the spin-dependent transmission. This approach will be justified by estimating the strength of electron-electron interaction in single channel semiconductor devices.

Here, we consider a narrow ballistic wire that is submitted to spin-orbit coupling with the Rashba term being dominant. In order to obtain a spin-polarized beam of electrons propagating in one direction, a small Zeeman field is introduced.³ By confining it in the y direction with lateral gates, the problem becomes unidimensional and the Hamiltonian for a one-dimensional wire reads³

$$H_0 = \frac{p^2}{2m^*} \sigma_0 - \frac{\alpha \langle \mathcal{E}_z \rangle}{\hbar} p_x \sigma_y + \frac{\epsilon_Z}{2B} \vec{B} \cdot \vec{\sigma}, \quad (1)$$

where m^* is the effective mass, $\langle \mathcal{E}_z \rangle$ is the electric Rashba field perpendicular to the layer and α depends on the material used. \vec{B} is the magnetic field and ϵ_Z is the Zeeman energy. σ_0 is the identity matrix and $\vec{\sigma} = (\sigma_x, \sigma_y, \sigma_z)$ the usual Pauli matrices. The eigenvectors are thus the products of plane waves times a spinor. The eigenstates are

$$E = \frac{\hbar^2}{2m^*} [k_x^2 \pm 2\sqrt{\kappa_Z^4 + k_\alpha^2 k_x^2}], \quad (2)$$

where $\kappa_Z^2 = (m^*/\hbar^2)(\epsilon_Z/2)$ and $k_\alpha = (m^*/\hbar^2)\alpha\langle \mathcal{E}_z \rangle$. The Rashba energy is defined through $E_\alpha = (\hbar^2/2m^*)k_\alpha^2$. The orientation of eigenvectors is such that for $E \gg E_\alpha$, the spinor associated to the mode with larger wave vector is directed along $|\uparrow\rangle_y$. In the interval $[E_\alpha - \epsilon_Z/2, E_\alpha + \epsilon_Z/2]$, there is only one propagating mode (with two chiralities). The other mode is evanescent. The dispersion relation for the propagating mode is indicated in Fig. 1. The existence of a pseudogap in a given energy interval has been used in Ref. 3, to propose a spin-filtering device, where a potential step of height V_1 corresponding to a gate voltage permits us to shoot in the middle of the pseudogap (Fig. 1).

Electron-electron interactions are taken into account, with $V_{\text{int}}(x)$, the Coulomb interaction potential. Following Ref. 11, which discusses the effect of weak electron interactions in a single mode 1D wire, we use a Hartree-Fock approach followed by a poor man's Anderson renormalization in energy space. The Dyson equation in Hartree-Fock approximation reads

$$\begin{aligned} \vec{\psi}_k(x) = & \vec{\phi}_k(x) + \int dy G_k^r(x, y) V_H(y) \vec{\psi}_k(y) \\ & + \int dy \int dz G_k^r(x, y) V_{\text{ex}}(y, z) \vec{\psi}_k(z), \end{aligned} \quad (3)$$

with $\vec{\psi}_k(\vec{\phi}_k)$ the one-electron wave function in the presence (absence) of interactions, and $G_k^r(x, y)$ is the retarded Green

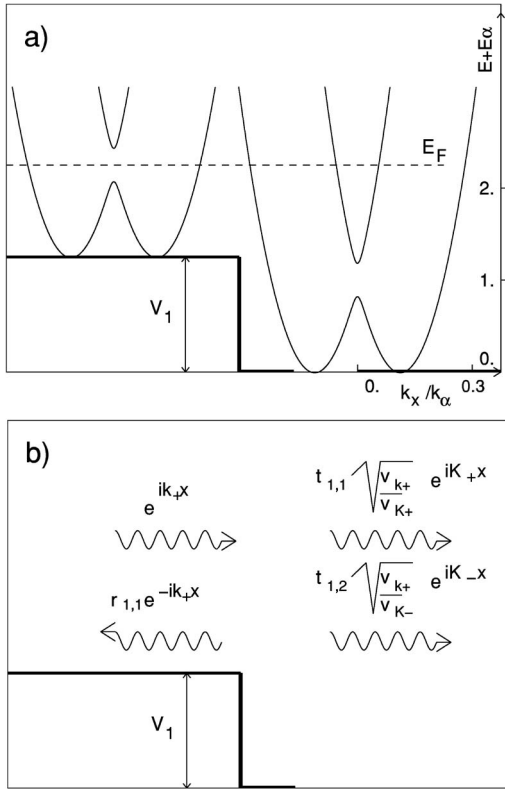


FIG. 1. (a) The thin lines denote the energies $E + E_\alpha$ of the two Rashba bands as a function of wave-vector ratio k_x/k_α both on the left of the potential step and on the right, for $\eta=0.3$ and $\Gamma=1.5$. The potential step of height V_1 is indicated as a thick line. The dashed line is the Fermi energy E_F . (b) One of the three scattering states. An incident wave e^{ik_+x} is injected on the left-hand side of the step and generates two transmitted waves and one reflected wave.

function. $V_H(x) = \int dy V_{\text{int}}(x-y)n(y)$, is the Hartree potential, with

$$n(y) = \sum_{n=1}^2 \sum_{|q| < k_{F(n)}} |\tilde{\psi}_q^n(y)|^2 \quad (4)$$

the local density. Note that the sum is carried over the two modes $\tilde{\psi}_q^n$ (propagating and evanescent), for all wave vectors q with energies smaller than E_F (at $T=0$). $k_{F(n)}$ are the wave vectors of modes n at the Fermi energy. The exchange potential (Fock) is given by the matrix

$$V_{\text{ex}}(x, y) = -V_{\text{int}}(x - y) \times \sum_{n=1}^4 \sum_{|q| < k_{F(n)}} \begin{pmatrix} \psi_{q,u}^{n*}(y) \psi_{q,u}^n(x) & 0 \\ 0 & \psi_{q,d}^n(y) \psi_{q,d}^{n*}(x) \end{pmatrix}, \quad (5)$$

where $\psi_{q,u}^n$ and $\psi_{q,d}^n$ are the components of $\tilde{\psi}_q^n(x)$ in the basis $\{|\uparrow\rangle_z, |\downarrow\rangle_z\}$. Assuming a finite range d for the Coulomb interaction, we will consider in our perturbative calculation only the terms in Eq. (3), which give the leading logarithmic divergence for the scattering coefficients at the Fermi level, as in Ref. 11.

In the case where the Fermi level lies in the middle of the pseudogap (Fig. 1), there are three scattering states. The first one corresponds to injecting electrons from the left of the step with an incident wave of wave-vector k_+ and group velocity v_{k_+} , thus generating a reflected wave of amplitude $r_{1,1}$ and two transmitted waves, $t_{1,1}\sqrt{v_{k_+}/v_{K_+}}e^{iK_+x}$ and $t_{1,2}\sqrt{v_{k_+}/v_{K_-}}e^{iK_-x}$, K_+ being the larger wave vector. The two other diffusion states are obtained by injecting electrons from the right of the step with wave-vector K_i ($i=+$ or $-$), thus generating reflected waves of the form $r'_{i,j}\sqrt{v_{K_i}/v_{K_j}}e^{iK_jx}$ and transmitted waves $t'_{i,1}\sqrt{v_{K_i}/v_{k_+}}e^{-ik_+x}$, $j=+$ or $-$. The square root factors insure the unitarity of the S matrix.¹²

In the geometry of Fig. 1, the S matrix thus takes the form

$$S = \begin{pmatrix} r_{1,1} & t'_{1,1} & t'_{2,1} \\ t_{1,1} & r'_{1,1} & r'_{2,1} \\ t_{1,2} & r'_{1,2} & r'_{2,2} \end{pmatrix}. \quad (6)$$

We introduce the physical parameter $\eta \equiv \sqrt{\epsilon_Z/E_\alpha}$, which is related to the ratio of the Zeeman energy to the Rashba energy. The other relevant parameter is the ratio

$$\Gamma = \sqrt{\frac{E_F}{E_\alpha}}, \quad (7)$$

where E_F is the energy of the Fermi level measured as in Fig. 1(a). In our case, E_F is connected to the height V_1 of the step. In order to inject electrons from the left, in the middle of the pseudogap, E_F must be equal to $E_\alpha + V_1$. Next, in order to have four propagating modes at the right of the step as in Fig. 1, V_1 must be larger than $\epsilon_Z/2$. Thus, the minimum value of Γ is $\sqrt{1 + \epsilon_Z/2E_\alpha}$. If $\eta \rightarrow 0$, $\Gamma \rightarrow 1$. In the renormalization procedure, following the usual procedure,¹³ one then rescales the bandwidth from D_0 , the real bandwidth, to D . Here D_0 is assumed to be larger than the step height V_1 . One then obtains flow equations for the quantities $t_{1,1}$, $t_{1,2}$, $t'_{1,1}$, and $t'_{2,1}$. It is more convenient to use $\tilde{t}_{i,j} = t_{i,j}\sqrt{v_{k_+}/v_{K_j}}$, and $\tilde{t}'_{i,1} = t'_{i,1}\sqrt{v_{K_i}/v_{k_+}}$. As an example, we quote the equation for $\tilde{t}_{1,1}$,

$$\frac{d\tilde{t}_{1,1}}{d \ln\left(\frac{D_0}{D}\right)} = -(\hbar\bar{v}_K)^{-1} \left[\tilde{t}_{1,1}|\tilde{r}'_{2,1}|^2 \left(\frac{v_{K_+}}{v_{K_-}}\right) + \tilde{t}_{1,2}r'_{1,1}\tilde{r}_{1,2}^* \right] \mathcal{J}'_1, \quad (8)$$

where $\bar{v}_K = \frac{1}{2}(v_{K_+} + v_{K_-})$. The integral \mathcal{J}'_1 is defined as $\mathcal{J}'_1 = \mathcal{J}'_1 - \mathcal{J}'_0$, where

$$\mathcal{J}'_0 = -\frac{v_{K_-}}{2\bar{v}_K} \hat{V}(K_{F+} + K_{F-}) \ln \left| \{(K_+ + K_-) - (K_{F+} + K_{F-})\} \frac{d}{2} \right|, \quad (9)$$

$$\mathcal{T}'_1 = -\frac{v_K}{2\bar{v}_K} \hat{V} \left(\frac{(K_+ - K_{F+}) + (K_- - K_{F-})}{2} \right) \times \ln \left| \left\{ (K_+ - K_{F+}) + (K_- - K_{F-}) \right\} \frac{d}{2} \right|, \quad (10)$$

where $\hat{V}(k)$ denotes the Fourier transform of V_{int} . The renormalization equations for $\tilde{t}_{1,2}$, $\tilde{t}'_{1,1}$, and $\tilde{t}'_{2,1}$ have a similar structure. $\mathcal{J}'_1 > 0$ for repulsive interactions.

Any S matrix can be written as $\exp(-i\vec{u} \cdot \vec{\lambda})$ with \vec{u} an eight-dimensional real vector and the components of $\vec{\lambda}$ are real matrices $[\text{SU}(3)]$. Since $\tilde{t}_{1,1}$, $\tilde{t}_{1,2}$, $\tilde{t}'_{1,1}$, and $\tilde{t}'_{2,1}$ are generally complex numbers, our renormalization equations give eight relations for real parameters and thus completely determine the flow of the S matrix. We now focus on the limit $\eta \rightarrow 0$ (small Zeeman coupling). The S matrix then simplifies and becomes a real and symmetric matrix

$$S = (\Gamma + 1)^{-1} \begin{pmatrix} \frac{(\Gamma - 1)^2}{\Gamma + 1} & 2\sqrt{\Gamma} & -2\sqrt{\Gamma} \frac{\Gamma - 1}{\Gamma + 1} \\ 2\sqrt{\Gamma} & 0 & \Gamma - 1 \\ -2\sqrt{\Gamma} \frac{\Gamma - 1}{\Gamma + 1} & \Gamma - 1 & 4 \frac{\Gamma}{\Gamma + 1} \end{pmatrix}. \quad (11)$$

It has a determinant of -1 instead of $+1$ because the number of propagating modes is not the same on each side. The S matrix stays real symmetric under the renormalization group flow and thus only two real equations for $t_{1,1}$ and $t_{1,2}$ are needed.

When injecting electrons from the left of the step (exactly in the middle of the pseudogap as in Ref. 3), one defines the polarization of the outgoing beam as

$$p = \frac{|t_{1,1}|^2 - |t_{1,2}|^2}{|t_{1,1}|^2 + |t_{1,2}|^2}. \quad (12)$$

The value $p=0$ corresponds to a totally unpolarized beam (experimentally not desirable). The value $p=1$ corresponds to a perfectly polarized outgoing beam. According to Eq. (11), p is simply Γ^{-1} . It tends to zero as the height of the step gets large with respect to the Rashba energy. The propagating modes are either oriented along the $|\uparrow\rangle_y$ or along the reverse direction.

Let $l = \ln(D_0/D)$ be the renormalization parameter and $A = \mathcal{J}'_1 / (2\pi\hbar\bar{v}_K)$. It is easier to express the renormalization group equations in terms of the variables $x = t_{1,1}^2 + t_{1,2}^2$ and $y = t_{1,1}^2 - t_{1,2}^2$. They read

$$\frac{dx}{dl} = -A(x^2 - y^2)\sqrt{1-x}(1-\sqrt{1-x}), \quad (13)$$

$$\frac{dy}{dl} = -\frac{1}{2}A(x^2 - y^2)y. \quad (14)$$

There are only three fixed points. The stable fixed point $x=0$, $y=0$ corresponds to a perfectly reflecting step; both $t_{1,1}$ and $t_{1,2}$ are zero. The unstable fixed point $x=y=1$ corresponds to $t_{1,1}=1$ and $t_{1,2}=0$, i.e., perfect transmission with no mode conversion. The second unstable fixed point

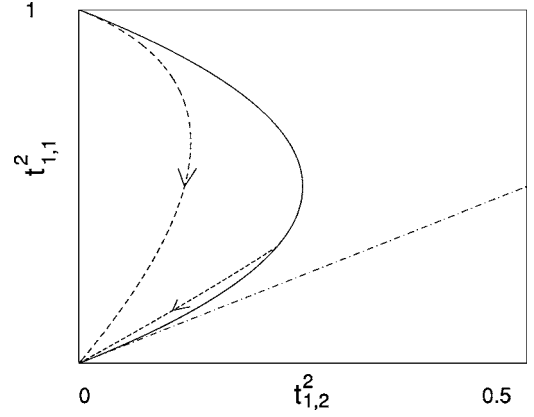


FIG. 2. Solid line: location of the initial points. Upper dashed line: renormalization group flow for $\Gamma=1$. The starting point is at $t_{1,1}=1$. Lower dashed line: renormalization group trajectory for $\Gamma=10$. The dashed-dotted line is simply the first diagonal, corresponding to totally unpolarized beams and reaches $t_{1,1}^2=1$ at $t_{1,2}^2=1$.

$x=1$, $y=-1$ corresponds to $t_{1,2}=-1$ and $t_{1,1}=0$ (complete mode conversion). When we have no electron-electron interactions, the location of the points where one starts the renormalization procedure, in the plane $(t_{1,2}^2, t_{1,1}^2)$, depends on one parameter only, Γ . Thus, the ensemble of points where one starts is a curve in this plane, which is represented in Fig. 2 as a solid line. In addition, the behavior of some flow trajectories is depicted in this figure.

We describe what happens first, if the height of the step is small with respect to the Rashba energy, second, in the reverse situation.

In the first case, Γ is barely larger than 1 (1 ideally). We then start from an initial temperature (bandwidth) $T_{\text{in}} = D_0/k_B$, where $t_{1,1}$ is close to 1 and $t_{1,2}$ close to zero, which means a perfect polarization of the outgoing beam. The point moves first in a direction such that the polarization diminishes significantly but the total transmission remains approximately constant. Then, the curve bends downwards and eventually moves towards the origin (no transmission). The polarization goes to a constant value.

In the second case (not desired in practice), Γ is large; the initial polarization is already low (equal to $2/\Gamma$) and still decreases towards a constant value. The transmission goes quickly to zero.

The renormalization procedure must be interrupted at some stage given by $D \approx k_B T$. In the case where Γ is close to 1 (small potential step), Eqs. (13) and (14) show that the total transmission first decreases very slowly as $1 - r_{\text{in}}^2 - 8r_{\text{in}}^2 A \ln^2(T/T_{\text{in}})$, where r_{in} is the initial reflexion coefficient. r_{in} goes to zero as Γ goes to 1. The polarization decreases as $\ln(T_{\text{in}}/T)$. For lower temperatures, the polarization goes to a constant Γ dependent value, which is equal to $1/2$ for $\Gamma=1$. The total transmission goes to zero, asymptotically like $\ln(T_{\text{in}}/T)^{-1/2}$, but this regime is only attained for unrealistic values of temperatures.

A characterization of such a spin filter requires the comparison of both the total transmission coefficient, together

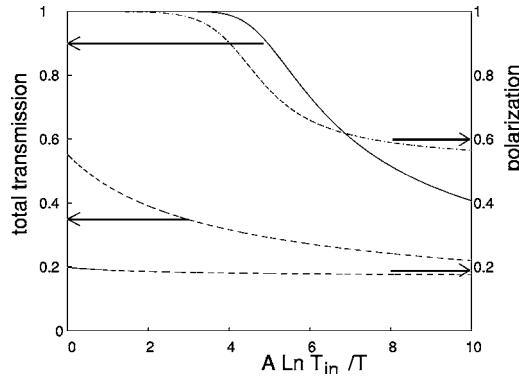


FIG. 3. Total transmission and polarization as a function of the logarithm of the temperature. The two curves marked with left arrows represent the total transmission for $\Gamma=1.01$ (solid line) and $\Gamma=10$ (dashed line). The two other curves represent the spin polarization for $\Gamma=1.01$ (dash-dotted line) and $\Gamma=10$ (dashed line), respectively.

with the evolution of the polarization under renormalization group flow. This information is illustrated in Fig. 3, where both quantities are plotted as a function of the logarithm of the inverse temperature. For Γ close to 1, the total transmission stays constant and close to unity until the temperature is dropped by several orders of magnitude, and then decreases in a monotonous fashion. At the same time, the polarization drops faster than the total transmission, signifying that the quality of the spin-filtering effect is polluted by electronic interactions before the total transmission is truly affected. For large Γ , the total transmission first decreases monotonously (linear behavior in $\ln T$) starting from the initial bandwidth, then giving place to a slower decrease $[(\ln T)^{-(1/2)}]$. The polarization stays approximately constant in this case, but at a deceptively low value of 0.2.

A useful way to quantify electron interactions is to compute the Luttinger parameter g , which is expected for a gated heterostructure. To be specific we consider the geometry of Ref. 14, where the Coulomb interaction in the 1D channel is screened by the few transverse modes in the wire and by the proximity of the two-dimensional electron gas (2DEG) and

gates: $V(r) \approx (e^2/4\pi\epsilon_0\epsilon)e^{-r/\lambda_s}/r$ ($\lambda_s \sim 100$ nm, comparable to the width of the wire, $W \sim 20$ nm). Averaging over the lateral dimensions of the wire, one obtains an effective one-dimensional potential. The Luttinger parameter g is then related to the zero-momentum Fourier transform of this potential $g = [1 + 4\tilde{V}(0)/\hbar v_F]^{-1/2}$. g increases with the ratio W/λ_s . Taking $v_F \sim 10^6$ m/s one obtains $g \approx 0.69$, which is remarkably close to the value of Ref. 14. It is also reasonably close to the noninteracting value 1. The materials used in Ref. 14 differ from the existing Rashba devices,¹⁵ but the typical parameters are comparable.

To summarize, we have looked at the effect of weak electron-electron interactions in one dimensional ballistic quantum wires under the combined Rashba and Zeeman effects. At the single electron level this device has the advantage of working as a spin filter. We have characterized the influence of electron-electron interactions in this same device. We found that in the most relevant case ($E_F - E_\alpha \ll 1$) where the total transmission remains close to unity for a range of bandwidths, the quality of spin-filtering properties decreases substantially. Although the present paper deals with a sharp step, the present approach can be extended to steps whose extension is much larger than the Fermi wave length, using WKB-type approximations. Transmission through the step is likely to be enhanced in this case, but the tendency for interactions to spoil filtering will remain valid. Also, this single electron picture can be further complicated in practice: For the case where two spin orientations are present (on the right-hand side of the step), it was shown¹⁶ that the combined effect of spin-orbit coupling and strong electron-electron interactions provide some limitations to the Luttinger liquid (metallic) picture, giving rise to spin- or charge-density wave behavior instead. Nevertheless, the present perturbative treatment of the Coulomb interaction is justified here because the one dimensional wire is surrounded by nearby metallic gates in order to implement the Rashba effect.

We thank P. Středa and F. Hekking for useful discussions and comments. This work is financially supported by CNRS A. C. Nanosciences.

¹*Towards the Controllable Quantum States*, Proceedings of the MS +S2002 Conference, Atsugi, Japan, 2002, edited by H. Takayanagi and J. Nitta (World Scientific, Singapore, 2003).

²*In the Light of Quantum Computation*, Proceedings of the MS +S2004 Conference, Atsugi, Japan, 2004, edited by H. Takayanagi and J. Nitta (World Scientific, Singapore, 2005).

³P. Středa and P. Šeba, Phys. Rev. Lett. **90**, 256601 (2003).

⁴S. Datta and B. Das, Appl. Phys. Lett. **56** (7), 665 (1990).

⁵E. I. Rashba, Fiz. Tverd. Tela (Leningrad) **2**, 1224 (1960) [Sov. Phys. Solid State **2**, 1109 (1960)]; Y. A. Bychkov and E. I. Rashba, J. Phys. C **17**, 6039 (1984).

⁶J. C. Egues, C. Gould, G. Richter, and L. W. Molenkamp, Phys. Rev. B **64**, 195319 (2001).

⁷V. F. Motsnyi, J. De Boeck, J. Das, W. Van Roy, G. Borghs, E. Goovaerts, and V. I. Safarov, Appl. Phys. Lett. **81**, 265 (2002).

⁸E. I. Rashba, Phys. Rev. B **62**, R16267 (2000).

⁹J. Schliemann and D. Loss, Phys. Rev. B **68**, 165311 (2003).

¹⁰A. V. Moroz, K. V. Samokhin, and C. H. W. Barnes, Phys. Rev. Lett. **84**, 4164 (2000); Phys. Rev. B **62**, 16900 (2000); A. Iucci, *ibid.* **68**, 075107 (2003).

¹¹K. A. Matveev, Dongxiao Yue, and L. I. Glazman, Phys. Rev. Lett. **71**, 3351 (1993); Dongxiao Yue, L. I. Glazman, and K. A. Matveev, Phys. Rev. B **49**, 1966 (1994).

¹²M. Büttiker, Y. Imry, and M. Y. Azbel, Phys. Rev. A **30**, 1982 (1984).

¹³C. L. Kane and M. P. A. Fisher, Phys. Rev. Lett. **72**, 724 (1994).

¹⁴O. M. Auslaender *et al.*, Science **295**, 825 (2002).

¹⁵J. Nitta, T. Akazaki, H. Takayanagi, and T. Enoki, Phys. Rev. Lett. **78**, 1335 (1997).

¹⁶V. Gritsev, G. Japaridze, M. Pletyukhov, and D. Baeriswyl, Phys. Rev. Lett. **94**, 137207 (2005).